Journal of Physiology (2002), **539.1**, *pp.* 253–266
DOI: 10.1013/jphysiol.2001.012728

www.jphysiol.org

Calcium release and intramembranous charge movement in frog skeletal muscle fibres with reduced (< 250 μM) calcium content

Paul C. Pape and Nicole Carrier

Département de physiologie et biophysique, Université de Sherbrooke Faculté de médicine, 3001, 12e Avenue Nord, Sherbrooke (*Québec*) *Canada J1H5N4*

It is generally accepted that activation of voltage sensors in the T-tubular membranes is a critical step of excitation–contraction coupling in skeletal muscle. The purpose of this study was to evaluate further whether the Q_γ component (delayed 'hump' component) of the intramembranous charge movement current (I_{cm}) results from movement of these voltage sensors. Ca^{2+} release and I_{cm} were measured in voltage-clamped frog cut fibres mounted in a double Vaseline-gap chamber. In order to reduce effects of Ca^{2+} feedback mechanisms, the calcium content of the sarcoplasmic reticulum (SR) during rest was reduced to < 250 μM (referred to volume of myoplasm) and maintained approximately constant. The early (Q_β) and Q_γ components of charge movement were estimated by fitting the sum of two Boltzmann functions to the total steady-state intramembranous charge *vs.* voltage data. The average voltage steepness factor (k) and half-maximal voltage ($\bar{V}$) for Q_γ were 4.3 and −57.4 mV (n = 6), respectively. The SR membrane permeability for Ca^{2+} release was assessed when a constant amount of calcium remained in the SR (usually about 60 μM). A single Boltzmann function fitted to these data gave values on average for k and $\bar{V}$ of 4.7 and −45.3 mV, respectively. The similarity of the values of k for Q_γ and Ca^{2+} release supports the idea that Q_γ reflects movement of voltage sensors for Ca^{2+} release. The greater value of $\bar{V}$ for Ca^{2+} release compared to Q_γ is consistent with multi-state models of the voltage sensor involving movement of Q_γ charge during non-activating transitions.

(Resubmitted 14 May 2001; accepted after revision 15 November 2001)

Corresponding author P. C. Pape: Département de physiologie et biophysique, Université de Sherbrooke Faculté de médicine, 3001, 12e Avenue Nord, Sherbrooke (Québec) Canada J1H5N4. Email: ppape01@courrier.usherb.ca

In 1973, Schneider & Chandler identified a non-linear capacitative current termed intramembranous charge movement (I_{cm}) and proposed that it results from the movement of voltage sensors from a resting state to a state that activates Ca^{2+} release from the sarcoplasmic reticulum (SR). Later, Adrian & Peres (1979) identified two components of I_{cm}, I_β and I_γ. I_β peaks early and decays with an approximately exponential time course whereas I_γ has a somewhat complex time course, usually appearing as a delayed 'hump' at intermediate voltages. Several results suggest that the I_γ component is associated with voltage activation of Ca^{2+} release including the observations that its steep voltage dependence (Hui & Chandler, 1990, 1991) is similar to that of tension (Hodgkin & Horowicz, 1960) and Ca^{2+} release (Miledi *et al.* 1981; Baylor *et al.* 1983; Maylie *et al.* 1987; Klein *et al.* 1996), and becomes prominent close to the mechanical threshold. Like Ca^{2+} release, it is reduced or eliminated by pharmacological agents such as tetracaine (Huang, 1982; Hui, 1983; Vergara & Caputo, 1983).

One possibility first suggested by W. K. Chandler (cited in Horowicz & Schneider, 1981) is that Ca^{2+} released from the SR binds to sites on the inner surface of the T-system membrane resulting in a depolarised surface potential thereby driving the movement of additional charge. In a series of articles (Csernoch *et al.* 1991; García *et al.* 1991, Szucs *et al.* 1991; Pizarro *et al.* 1991), Ríos and colleagues proposed that Q_γ is not a separate component of charge, rather that it is Q_β charge moved in response to such a calcium-induced local depolarisation. (Q_γ and Q_β are amounts of intramembranous charge obtained by integration of I_γ and I_β, respectively.)

In contrast to this idea, results from W. K. Chandler's laboratory indicate that the Q_γ 'hump' component is still present and that steady-state charge *vs.* voltage data are essentially unchanged when calcium is removed from the SR thereby essentially eliminating Ca^{2+} release (Jong *et al.* 1995*b*; Pape *et al.* 1996). In addition, Ca^{2+} release, measured at low levels of depolarisations (−80 to −57 mV) and in the presence of a large concentration of the Ca^{2+} buffer EGTA, has a steep voltage dependence similar to that of Q_γ (Pape *et al.* 1995). Under these conditions, Ca^{2+} from one voltage-activated site should not have influenced the state of activation of essentially all neighbouring voltage-activated sites due to the relatively large average

distance between sites and the buffering action of EGTA. Pape *et al.* (1995) concluded that the steep voltage dependence of Ca^{2+} release is due to the intrinsic properties of the voltage sensors rather than an effect of Ca^{2+} release on Q_β or some other process.

Although the results cited above suggest a correlation between Q_γ and Ca^{2+} release, they do not prove a cause and effect relationship between the two processes. One problem is that the steep voltage dependence of Ca^{2+} release and tension were obtained with relatively small depolarisations, in a voltage range in which Q_γ is small and not clearly distinguished from the Q_β component, whereas the steep voltage dependence of Q_γ was determined under different experimental conditions and from measurements at more positive voltages. Another problem is that results are difficult to interpret at more positive potentials, when Q_γ is prominent, due in large part to feedback effects of Ca^{2+} release on the kinetics of Q_γ (Jong *et al.* 1995*b*; Pape *et al.* 1996) and on the SR Ca^{2+} release channel itself. The most studied of these feedback mechanisms is calcium inactivation of Ca^{2+} release (Baylor *et al.* 1983; Schneider & Simon, 1988). It was estimated that at least 90 % of the ability of a fibre to release Ca^{2+} is impaired by an action potential or by a 10–15 ms pulse to −20 mV under voltage clamp conditions, even in the presence of 20 mM EGTA in the internal solution (Jong *et al.* 1995*a*). This indicates that the ability of a fibre to release Ca^{2+} is already greatly reduced by the time to peak of a rate of Ca^{2+} release signal elicited by moderate to large depolarisations. In addition, only a fraction of the steady-state Q_γ charge moves by this time to peak, further confounding the problem of evaluating a possible correlation between Ca^{2+} release and Q_γ. The strategy in this study was to remove most of the calcium from the SR in order to eliminate or greatly reduce calcium inactivation and also an inhibitory effect of Ca^{2+} release on the kinetics of Q_γ (Pape *et al.* 1996) while leaving enough so that Ca^{2+} release could still be detected. The main aim was to compare Ca^{2+} release with steady-state Q_γ charge over the full voltage range from −70 to +10 mV.

METHODS

The experimental procedures were essentially the same as those described previously (Pape *et al.* 1995, Pape & Carrier, 1998). Briefly, cold-adapted frogs (*Rana temporaria*) were killed by decapitation and spinal cord destruction with protocols approved by the Comité d'éthique de l'expérimentation animale at the Université de Sherbrooke. Cut twitch fibres (Hille & Campbell, 1976) isolated from semi-tendinosus or ileo-fibularis muscles were stretched to a sarcomere length of 3.5–3.9 μm and mounted on a double Vaseline-gap chamber maintained at 14–16 °C. The membranes in the end pools were made permeable by a 2 min exposure to 0.01 % saponin in a caesium glutamate internal solution (see below). The voltage in one end pool, denoted V1, was clamped by passing current at the other end pool and collecting it with a bath clamp that maintains the central pool at the ground potential. A holding current maintained fibres at a resting potential of −90 mV. The EGTA–Phenol Red method (Pape *et al.* 1995) was used to estimate Ca^{2+} release. Briefly, the total amount of Ca^{2+} released from the SR in response to stimulation is given by:

$$\Delta[Ca_T] = \beta/2\Delta pH,$$

where $\Delta[Ca_T]$ refers to myoplasmic volume, β is the buffering power of myoplasm in cut fibres which is taken to be 22 mM (pH unit)$^{-1}$, and ΔpH is the pH change measured with the absorbance indicator Phenol Red. Pape & Carrier (1998) gives details relating to the measurement of ΔpH with our apparatus. The rate of Ca^{2+} release is given by $d\Delta[Ca_T]/dt$. The amount of calcium present at the start of a stimulation, denoted $[Ca_{SR}]_R$ (the subscript R denotes resting), is given by the maximum of the $\Delta[Ca_T]$ signal after a strong depolarisation that releases essentially all the calcium from the SR. The amount of calcium in the SR at any time during a stimulation, denoted $[Ca_{SR}]$, is given by $[Ca_{SR}]_R - \Delta[Ca_T]$. The release permeability is given by $d\Delta[Ca_T]/dt$ divided by $[Ca_{SR}]$ and multiplied by 100 to give percentage of SR calcium content released per millisecond. The release permeability provides an estimate of the extent of activation of SR Ca^{2+} release channels since the driving force for Ca^{2+} release should be approximately proportional to $[Ca_{SR}]$. This follows since $[Ca^{2+}]$ in the SR should be approximately proportional to the SR calcium content during Ca^{2+} release since calsequestrin complexes calcium with low affinity (MacLennan & Wong, 1971) and with rapid kinetics (time constant < 1 ms; Prieto *et al.* 1994; Donoso *et al.* 1995). In addition, since calsequestrin is the major source of calcium (estimated to be ~92 % of total SR Ca^{2+} in partially depleted fibres; from Donoso *et al.* 1995, assuming that terminal cisternae comprise 40 % of total SR volume; Mobley & Eisenberg, 1965) and it is localised near the release sites in the terminal cisternae, diffusional delays should be minimal.

Composition of the internal and external solutions

The end pools contained (mM): 45 caesium glutamate, 20 EGTA as a combination of the caesium salt and, if Ca^{2+} was present, the Ca^{2+} salt; 6.8 $MgSO_4$, 5 Cs_2-ATP, 20 caesium creatine phosphate, 5 caesium phospho(enol)pyruvate, and 5 3-[*N*-morpholino]-propanesulfonic acid (Mops). The solution with Ca^{2+} present contained 0.70 mM total calcium, which is 40 % of the amount used to obtain a nominally normal amount of calcium load of the SR (one experiment used 50 % instead of 40 %, fibre ID 901991). The pH of the internal solutions (with or without Phenol Red) was adjusted to 7.0 at room temperature. (Measurements made at a later date indicate that the solutions were actually ~7.05 at 15 °C). The calculated concentrations of free calcium (if present) and free magnesium were 12 nM and 0.6 mM, respectively. The central pool solution contained (mM) 110 TEA-Cl, 10 $MgSO_4$, 10 Mops and 1 μM tetrodotoxin (TTX). Its pH was 7.1 and it was nominally Ca^{2+} free. After initial optical measurements, the end-pool solution was exchanged for one containing Phenol Red with a nominal concentration of 1 mM.

Intramembranous charge movement

The first step in estimating intramembranous charge movement is to measure an $I_{test} - I_{control}$ signal; Chandler & Hui (1990) and Hui & Chandler (1990) describe various aspects of these measurements. Briefly, $I_{control}$ is measured between −110 and −90 mV and it contains capacitative and ionic components and a small amount of intramembranous charge movement. This signal is scaled by the ratio of the change in voltage during the test to that during the control and subtracted from the I_{test} signal to yield the

$I_{test} - I_{control}$ signal, thereby correcting for linear capacitance and linear ionic components present in the I_{test} signal. An estimate of the intramembranous charge movement current, denoted I_{cm}, is obtained by subtracting non-linear ionic currents. The non-linear ionic current is estimated from a baseline, usually the average of the last 50 ms of the $I_{test} - I_{control}$ signal, multiplied by the voltage template. The voltage template is simply the voltage trace during the control, which has the same time course as the test voltage (confirmed for all the voltage pulses in this article), scaled to have a final amplitude of one. In the case of a constant baseline, therefore, the non-linear ionic component is assumed to have the time course of the voltage pulse.

In cases where non-linear ionic currents are absent or relatively small, it has been shown that the amount of charge moved during the OFF pulse (obtained from the integral of I_{cm} and denoted Q_{OFF}) is equal to the negative of the amount moved during the ON pulse. In general, estimates of Q_{OFF} are more reliable than those of Q_{ON} due to the fact that ON charge is slower and may contain non-linear ionic current with an unknown time course. Unless indicated otherwise, the amounts of total steady-state charge in this article are estimated from the OFF I_{cm} signals using constant baselines fitted to the end of the OFF pulses. It was of interest to obtain information during some ON pulses in this study. The approach used is described in Fig. 1*A* of Pape *et al.* (1996). Briefly, the baseline is a sloping line constrained to force the resulting Q_{ON} to equal $-Q_{OFF}$ and to pass through the end of the $I_{test} - I_{control}$ signal by minimising the sum of squares difference between the line and the last 50 ms of the $I_{test} - I_{control}$ signal. This correction minimises concerns relating to an apparent inequality between Q_{ON} and $-Q_{OFF}$ obtained by other methods for estimating the ON baseline in the presence of significant non-linear ionic current during an ON pulse.

Electrical parameters monitored during the experiment include holding current, apparent capacitance of the fibre (C_{app}), internal resistance per unit length of fibre (r_i), and capacitance (including surface and T-system membranes) per unit length of fibre (c_m). Details concerning the determination and definition of these parameters are given in Chandler & Hui (1990).

Filtration of signals

All the signals were filtered with a 1 kHz 4-pole Bessel filter. Except for Fig. 6, the optical traces only were filtered with a 0.1 kHz digital Gaussian filter (Colquhoun & Sigworth, 1983).

Statistical tests of significance

Two sets of results were considered to be significantly different if the Student's two-tailed t test parameter P was < 0.05. As explicitly stated in each case, the Student's paired t test was used to compare results from the same set of experiments.

RESULTS

Voltage protocol

The main aim of this study was to compare release permeability with intramembranous charge movement over a range of voltages. It was desirable to have

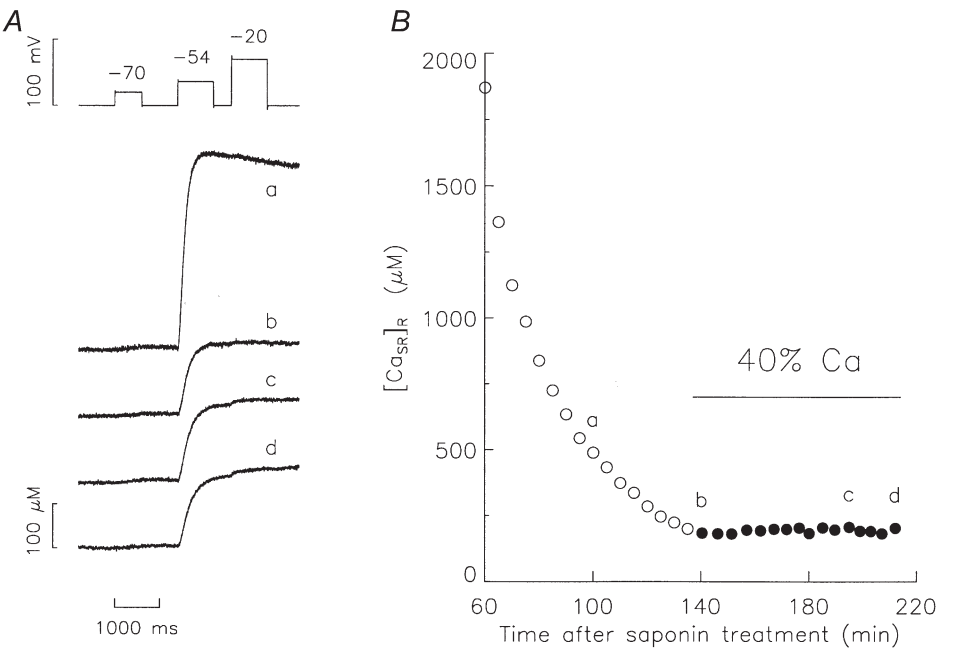

Figure 1. Illustration of stimulation protocol and $[Ca_{SR}]_R$ during an experiment

A, the top trace shows the change in V1 from the resting potential of −90 mV. The duration of the pulses to −70, −54, and −20 mV were 600, 800 and 800 ms, respectively. The duration of the periods at −90 mV at the start, between the 1st and 2nd pulses, and between the 2nd and 3rd pulses were 800, 800 and 400 ms, respectively. The bottom four traces show $\Delta[Ca_T]$ measured with the EGTA-Phenol Red method in response to this stimulation protocol at different times during the experiment. *B,* shows the time course of $[Ca_{SR}]_R$ plotted *vs.* time after saponin treatment of the fibre segments in the end pools. The end-pool solution initially contained no Ca^{2+}. As indicated by the horizontal bar and the filled symbols, the end-pool solution was exchanged for one containing 40 % of the Ca^{2+} used to obtain a nominally normal amount of calcium in the SR. The points labelled a-d were obtained from the similarly labelled $\Delta[Ca_T]$ traces in *A*. Fibre reference 915991, see legend of Table 1 for additional information.

approximately the same calcium content in the SR prior to each stimulation (denoted $[Ca_{SR}]_R$) at a relatively small value in order to eliminate or at least minimise the development of Ca^{2+} inactivation of Ca^{2+} release. Figure 1 illustrates the stimulation protocol and approach used to achieve these conditions. The top trace in *A* shows superimposed voltage records measured at four different times during the experiment. The protocol consisted of pulses to −70, −54, and −20 mV. The bottom four traces show the corresponding $\Delta[Ca_T]$ signals. One purpose of the final pulse to −20 mV was to insure that all the calcium was released from the SR; $[Ca_{SR}]_R$ was estimated as the maximum level of $\Delta[Ca_T]$. Figure 1*B* plots $[Ca_{SR}]_R$ *vs.* time after saponin treatment from the traces in *A* and other traces during the experiment. The open circles were obtained when no calcium was present in the internal solution. The horizontal line and filled circles indicate the period when calcium was present in the internal solution. The amount of calcium was 40 % of that used previously to approximate physiological calcium loading (see Methods). The other manoeuvre used to achieve approximately constant $[Ca_{SR}]_R$ values was to adjust the interval between stimulations to between 3.5 and 5.5 min, thereby varying the fraction of calcium pumped back into the SR following the preceding fully depleting stimulation. (As described in Pape *et al.* 1995, a period of 5 min provides enough time to pump back essentially all the recoverable calcium released by a fully depleting stimulation in the presence of 20 mM EGTA.) As seen by the filled circles, an approximately constant $[Ca_{SR}]_R$ was achieved.

All the stimulation protocols during the experiment were identical in terms of voltages and pulse durations to that described in *A* except that the voltage of the middle pulse, the test voltage, was varied during the period when calcium was present in the internal solution. In most experiments, the test pulse was preceded by a small pulse (typically −70 mV) used to monitor Ca^{2+} release when only a small fraction of channels were activated, thereby providing one means of evaluating whether long-term changes occurred during the series of measurements at different test voltages. The presence of this first small pulse should not have influenced the results during the test pulse (Pape & Carrier, 1998).

Intramembranous charge movement with the usual method for estimating ionic current

The top of Fig. 2*A* shows superimposed test voltage pulses from the experiment in Fig. 1 obtained after calcium had been added to the internal solution. The other traces in *A* show the corresponding $I_{test} - I_{control}$ signals at the voltages indicated. Between −54 and −45 mV, there is an early I_β component followed by a distinct delayed 'hump' component associated with the I_γ component (Adrian & Peres, 1979; Hui & Chandler, 1990). The traces at the more positive potentials show a very large, slowly developing outward current, which is similar in magnitude and voltage dependence to that reported by Hui & Chen (1994), also in the presence of 20 mM EGTA in the internal solution and Cl^- in the external solution. Hui & Chen attributed this current to a Ca^{2+}-independent Cl^- conductance. Figure 2*B* shows estimates of I_{cm} during the OFF pulse. Consistent with previous observations, the OFF I_{cm} traces have an early negative peak followed by a rapid decline to a final level. An important difference to note, however, is the initial apparent outward current in the estimated I_{cm} trace at 0 mV. An explanation for the initial spike discussed below is that the Cl^- current turns off after a delay.

The top trace in Fig. 2*C* shows the voltage step to −54 mV. The second trace shows the associated On $I_{test} - I_{control}$ signal from *A*. The line is the baseline used to estimate the non-linear ionic component obtained with the constraint that $Q_{On} = -Q_{OFF}$ (see Methods). The third trace shows the resulting I_{cm} signal on an expanded time scale. This signal shows an early peak followed by a rapid decline to near zero followed by an increase. As seen more clearly in the $I_{test} - I_{control}$ signal, the delayed increase appears to be due to the start of the Q_γ 'hump' component. This result suggests that all the early Q_β component moved before the Q_γ component started to appear. The ability to see an apparently clear kinetic distinction between Q_β and Q_γ can be attributed to a slowing of the kinetics of Q_γ with decreased Ca^{2+} release (Jong *et al.* 1995*b*). This apparent distinction provides a means of directly estimating Q_β and Q_γ. The estimated amount of steady-state Q_β charge at −54 mV; given by the area between the cursors in Fig. 2*C* normalised for linear capacitance; is 1.86 nC μF^{-1}. This value is used below. The time course of Q_γ charge movement, I_γ, is assumed to be the same as the I_{cm} signal (complete signal not shown) except with zero current during the first 23 ms (i.e. until the time of the 2nd cursor). This estimate of $I_\gamma(t)$ at −54 mV is used below with Fig. 6.

Peak values of the ON I_{cm} traces were used to estimate the voltage dependence of Q_β at relatively negative voltages, between −70 and −51 mV. The peak values were considered to be proportional to the steady-state Q_β charge moved, since the time courses of the I_{cm} traces are approximately the same up to the time when the current had decayed to half the peak value (assessed by superimposing the traces scaled to the same peak value; not shown). In addition, the contribution of the I_γ component at the time of the peak should be small on account of its delayed start and small magnitude at these relatively negative voltages. The filled circles in Fig. 2*D* plot the peak values *vs.* voltage. The curve is the least-squares fit of an exponential function to the data, which has an *e*-fold constant of 15.7 mV. This value is a direct estimate of the voltage steepness factor, *k*, of the Boltzmann function associated with Q_β (see eqn (1) in the next paragraph). This value is used below.

Separation of Q_γ and Q_β components by fitting two Boltzmann functions

The approach used to separate steady-state Q_γ and Q_β, first described by Hui & Chandler (1990), is to fit two Boltzmann functions to the total intramembranous charge *vs.* voltage data. They found a statistically significant improvement of the fit compared to a fit of just one Boltzmann function and concluded that the steeply voltage-dependent Boltzmann function is probably due to Q_γ. In support of this, the estimated voltage steepness was similar to values estimated with other methods used to isolate the Q_γ component (Hui & Chandler, 1991).

With the nomenclature of Hui & Chandler (1990), a single two-state Boltzmann distribution function of charge normalised by linear capacitance per unit length of fibre, c_m, is given by:

$$q/c_m = \frac{q_{max}/c_m}{1 + \exp(-(V - \bar{V})/k)}, \quad (1)$$

where q and q_{max} are the steady-state amounts of charge per unit length of fibre at voltage V and infinite voltage, respectively, $\bar{V}$ is the voltage at which half the charge is moved and k is the voltage-steepness factor.

The open circles in Fig. 3*A* plot the OFF charge associated with the I_{cm} traces in Fig. 2*B* and other traces from the same experiment. The smooth curve through the open circles shows the best fit of the sum of two Boltzmann distribution functions to the steady-state charge *vs.* voltage data with

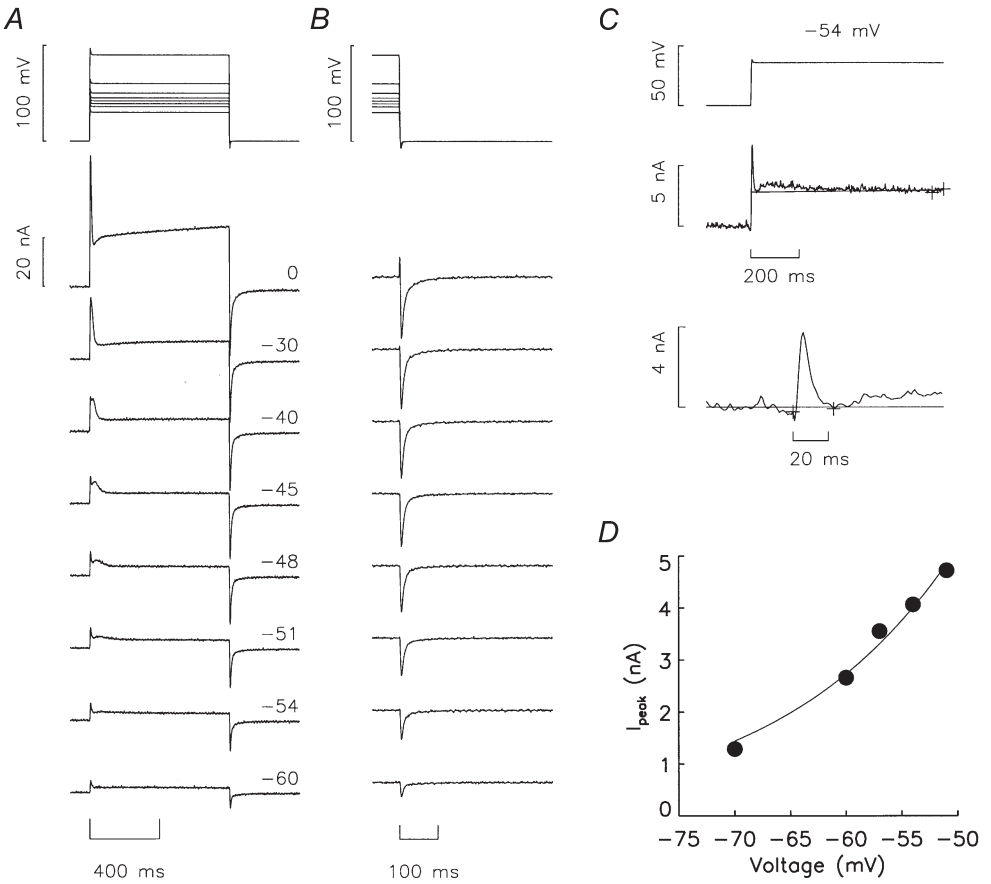

Figure 2. Intramembranous charge movement at different voltages

A, the top traces show different test voltage signals. The bottom traces show the corresponding $I_{test} - I_{control}$ signals obtained at the voltages indicated. *B*, the top traces show the same voltage signals as in *A* during the end of the ON pulse and all of the OFF pulses. The bottom traces show the corresponding I_{cm} signals during the OFF pulse obtained by subtracting estimates of ionic currents from the $I_{test} - I_{control}$ signals of *A*. The ionic currents here were determined with a constant baseline given by the average of the final 50 ms at the end of the pulses (see Methods). *C*, the top trace shows the voltage pulse to −54 mV. The next trace shows the corresponding $I_{test} - I_{control}$ signal. The line shows the baseline used to estimate the non-linear ionic current with the constraint that Q_{ON} equals $-Q_{OFF}$, which was 13.58 nC μF^{-1} (see Methods). The next trace is the resulting I_{cm} signal on an expanded time scale. The line shows the zero current level. The first and second cursors for the I_{cm} trace at −54 mV mark the start of the pulse and 23 ms later, respectively. *D*, the points plot *vs.* voltage the peaks of the I_{cm} trace in *C* and other traces obtained with voltage pulses between −70 and −51 mV. The curve is the best fit exponential function to this data; it had an e-fold voltage steepness factor of 15.7 mV. Same experiment as shown in Fig. 1.

'gap corrections' to take into account current flow under the Vaseline seals (Hui & Chandler, 1990). (The 'gap corrections' have little effect on the main parameters of interest in this study, k_γ and $\overline{V}_\gamma$; in the study of Hui & Chandler in 1990, the average value of k_γ was not changed by the 'gap correction' and the value of $\overline{V}_\gamma$ changed from −56.2 to −56.5 mV.)

Delay in the turn off of I_{Cl}

The delayed signal in the pair of traces in Fig. 3*B* shows the difference between the $I_{test} - I_{control}$ signal measured at +10 mV and that at 0 mV. This trace, designated $\Delta I_{test} - I_{control}$ (+10,0), should mainly reflect the difference between the non-linear ionic current at +10 mV compared to 0 mV since a relatively small difference in the charge movement currents is expected. The earlier trace is the voltage trace to +10 mV scaled to have the same initial and final steady levels as the $\Delta I_{test} - I_{control}$ trace. The $\Delta I_{test} - I_{control}$ trace has approximately the same time course as the voltage trace, but delayed by about 1.5 ms. A similar 1.5 ms delay was observed with more negative voltages though the relatively small ionic component compared to differences in intramembranous charge made it impossible to determine whether the same delay was present at voltages more negative than −30 mV. Similar delays (1.4 to 2.0 ms) were observed in all six experiments in this study. A likely explanation for the delays is that the Cl^- current turns off with the time course of the voltage trace delayed by at least 1.5 ms following repolarisation.

In order to evaluate whether a delay in the turn off of I_{Cl} influences the estimate of Q_γ, the ionic current was assumed to have the time course of the voltage trace delayed by 2 or 3 ms. The filled circles in Fig. 3*A* plot $-Q_{OFF}$ *vs.* voltage from I_{cm} traces obtained with the assumption that the OFF ionic current has the time course of the voltage pulse delayed by 3 ms. As seen by the close correspondence of the curve to the filled circles, the data is again well described by the sum of two Boltzmann distribution functions. Importantly, the imposition of a delay produces essentially no effect on the parameters for the Q_γ component (see discussion of Table 1 below). This is because possible errors in the time course of the ionic component appear to have little effect on Q_{OFF} for voltages more negative than −40 mV, the voltage range over which most of the change in Q_γ charge occurs (cf. open and filled circles in Fig. 3*A*). Three reasons indicate that the imposed delay provides a better estimate of the Q_β component. (1) The imposition of a delay eliminates the early initial outward spike in the OFF I_{cm} trace at the more positive potentials (e.g. 0 mV trace in Fig. 2*B*). (2) The amount of Q_β moved at −54 mV predicted from the fit to the filled circles is 1.80 nC μF^{-1}, which is very close to the direct estimate of 1.86 nC μF^{-1} described with Fig. 2*C*. (The fit to the open circles gave a value of 0.24 nC μF^{-1}.) (3) The value of k for the Q_β component from the fit to the filled circles, 18.7 mV, is also close to the direct estimate of 15.7 mV obtained with Fig. 2*D* above. (The fit to the open circles gave a value of 7.7 mV.) Similar improvements were

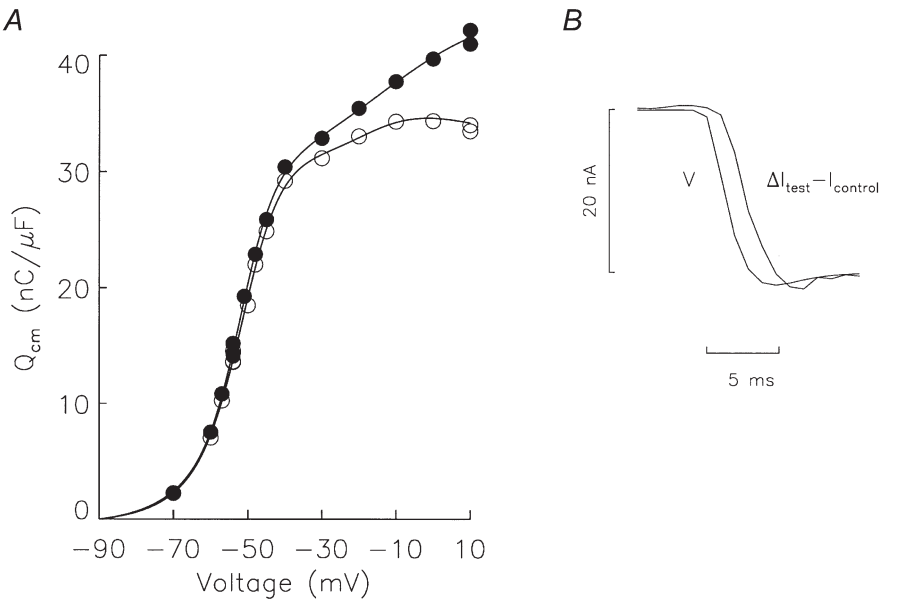

Figure 3. Q_{OFF} and delay in the turn off of I_{Cl}

A, ○s plot Q_{cm} *vs.* voltage data calculated as the negative values of the integrals of the OFF I_{cm} signals from Fig. 2*B* and signals at other voltages obtained in the same way. The curve shows the fit of two Boltzmann functions with 'gap corrections' to the charge *vs.* voltage data as described for Fig. 9B in Hui & Chandler (1990). The ●s and associated curve were obtained in the same way except that the OFF ionic current is assumed to turn off with a 3 ms delay (see text). *B*, the delayed signal is $\Delta I_{test} - I_{control}$(+10, 0) (see text). The early trace is the voltage pulse to +10 mV scaled to have the same change in amplitude as the $\Delta I_{test} - I_{control}$. Same experiment as shown in Figs 1 and 2.

obtained with a 2 ms delay. The 3 ms delay, however, produced a closer match to the directly estimated values of Q_γ (point 2) and k_β (point 3) in this and most of the other experiments. Both delays significantly improved the match compared to no delay in all of the experiments.

Summary of the charge movement results and fibre parameters

Table 1 summarises the parameters for Q_β and Q_γ obtained from the fit of two Boltzmann functions to the charge *vs.* voltage data for the six experiments in this study. The first section of the Table gives the results with no delay imposed on the OFF ionic current (cf. I_{cm} traces in Fig. 2*B*). The second and third sections were obtained with I_{cm} signals calculated with the assumption that the OFF ionic current turns off with a 2 and 3 ms delay, respectively. As noted above, the imposition of a delay had essentially no effect on the parameters of the Q_γ component. The conclusion from these results and the previous section is that the Q_γ component appears to be well determined in these experiments even though there is uncertainty in the Q_β component.

The legend of Table 1 gives fibre parameters at the start and end of the period during which the intramembranous charge measurements were obtained. With the exception of time after saponin treatment and the concentration of Phenol Red which are expected to vary, the values remained reasonably stable during the experiments. The values are not significantly different from those previously obtained under similar conditions (cf. Jong *et al.* 1995*b*; Pape & Carrier, 1998).

Release permeability when $[Ca_{SR}]$ is 60 μM

Figure 4 shows electrical and optical signals at several voltages. The top trace in *A* shows a voltage pulse to +10 mV. The next trace down shows the associated $\Delta[Ca_T]$ signal. The next trace shows the rate of Ca^{2+} release. The next trace is the release permeability, which is expected to be approximately proportional to the extent of activation of SR Ca^{2+} release channels (see Methods). The bottom trace shows the I_{cm} signal. Traces corresponding to those in A are shown in *B* for the pulse to −20 mV. An important thing to note is that the peaks of the $d\Delta[Ca_T]/dt$ and release permeability signals at −20 mV are similar to the corresponding peaks at +10 mV indicating that these signals approach their maximum by −20 mV. Figure 4*C* and *D* shows the corresponding results for −45 and −54 mV, respectively. There was a clear decrease with voltage in both the $d\Delta[Ca_T]/dt$ and release permeability signals.

Voltage dependence of Q_γ and Ca^{2+} release

The main aim of this study was to evaluate the relationship between the steady-state amount of Q_γ charge and the extent of activation of Ca^{2+} release channels over an extended voltage range from −70 to +10 mV. Since the release permeability is known to be sensitive to $[Ca_{SR}]$ in the range of $[Ca_{SR}]$ values present in these experiments (see Appendix), a narrow range of $[Ca_{SR}]$ values was chosen for the evaluation of release permeability. The first and second cursors in all the traces in Fig. 4 mark the ends of the range of $[Ca_{SR}]$ used in this experiment, 65 to 55 μM, respectively, determined from the $\Delta[Ca_T]$ trace. The range was chosen after almost all the charge movement associated with the Q_γ 'hump' component had apparently moved at each of the voltages tested but before $[Ca_{SR}]$ had

Table 1. Fit of two Boltzmann functions with gap correction to Q_{cm}(V) data

(1) Fibre	(2) k_β (mV)	(3) $\overline{V}_\beta$ (mV)	(4) $Q_{\beta,max}$ (nC μF^{-1})	(5) k_γ (mV)	(6) $\overline{V}_\gamma$ (mV)	(7) $Q_{\gamma,max}$ (nC μF^{-1})
No delay						
901991	9.4	−36.9	11.0	5.2	−58.3	21.3
913991	10.5	−8.7	7.5	3.8	−51.8	35.2
915991	7.7	−18.0	7.2	5.4	−52.5	36.4
921991	11.4	−37.7	11.8	4.6	−61.4	32.3
923991	8.9	−33.5	14.6	4.0	−67.3	32.1
420001	5.2	−29.5	18.0	2.8	−52.9	23.0
Mean	8.9	−27.4	11.7	4.3	−57.4	30.1
S.E.M.	0.9	4.7	1.7	0.4	2.5	2.6
OFF ionic current delayed 2 ms						
Mean	10.7	−24.0	17.7*	4.3	−58.0	30.1
S.E.M.	1.3	4.4	1.7	0.4	2.6	2.6
OFF ionic current delayed 3 ms						
Mean	14.3*†	−20.4*	25.3*†	4.2	−58.0*	29.4
S.E.M.	1.8	3.8	2.3	0.4	2.5	2.3

Column 1 gives the fibre reference. Columns 2–7 give the parameters from a fit of two Boltzmann functions to intramembranous charge *vs.* voltage data, taking into account current flow under the Vaseline seals. Columns 2–4 and columns 5–7 give the parameters indicated in the column headings for the Q_β and Q_γ components, respectively. The table is divided into three sections corresponding to the assumed time course of the ionic current. (See text for details.) * with mean values in the second and third sections indicate a statistically significant difference between the corresponding mean value in the first section (Student's paired *t* test; $P < 0.05$), and † in the third section have the same meanings between the corresponding mean values in the second section. Values at beginning and end of period in which voltage dependence of charge movement was determined for fibre reference 901991, 913991, 915991, 921991, 923991, and 420001, respectively: time after saponin treatment in min, 120–190, 113–200, 140–217, 178–261, 129–251, 88–159; holding current in nA, −28.7 to −46.5, −11.6 to −12.9, −31.0 to −34.0, −36.5 to −53.2, −43.8 to −49.5 and −34.8 to −80.1; concentration of Phenol Red in mM at optical site, 2.0–3.0, 2.1–2.5, 2.3–2.9, 2.2–2.4, 1.2–2.1, 1.4–1.8; resting pH, 6.62–6.53, 6.76–6.78, 6.61–6.62, 6.60–6.62, 6.53–6.51 and 6.72–6.53; C_{app} in μF, 0.0161–0.0163, 0.0126–0.0126, 0.0139–0.0143, 0.0138–0.0144, 0.0209–0.205 and 0.0175–0.0178; r_i in MΩ cm^{-1}, 4.16–4.66, 2.62–2.54, 3.11–3.11, 2.82–2.90, 2.61–2.47 and 2.08–2.35; c_m in μF cm^{-1}, 0.215–0.204, 0.182–0.182, 0.189–0.194, 0.188–0.188, 0.281–0.274 and 0.242–0.227. $[Ca_{SR}]_R$ range given in columns 2 and 3 of Table 2. Temperature 14–16 °C; sarcomere spacing 3.5–3.9 μm.

decreased to a level where noise became a serious problem. For the pulse to −45 mV, it is estimated that 95 % of the charge in the Q_γ 'hump' had moved by the time of the first cursor.

The smooth curve on the left in Fig. 5 shows the normalised Boltzmann function corresponding to the Q_γ component from the fit to the open circles in Fig. 3*A*. The filled circles plot, *vs.* voltage, the average release permeability when $[Ca_{SR}]$ was between 65 and 55 μM (see Fig. 4). The values are normalised by the maximum value of 3.85 % ms^{-1} estimated below. The most important thing to note is that the release permeability values have a steep voltage dependence similar to that of Q_γ charge and also appear to saturate at voltages above −30 mV. The release permeability data, however, appear shifted to the right by several millivolts.

The release permeability data in this and other experiments in this study are reasonably well described by a single Boltzmann function (cf. eqn (1)) with the following parameters: the maximum release permeability (denoted Rel_{max}), the half-maximal voltage (denoted $\bar{V}_{Rel}$), and the voltage steepness (denoted k_{Rel}). The value of k_{Rel} from the fit in Fig. 5 is 4.0 mV, which is similar to the value of 5.4 mV for the value k for the Q_γ component of charge movement. The value of $\bar{V}_{Rel}$ was −47.0 mV which is 5.5 mV more positive than the value of $\bar{V}$ for Q_γ.

Table 2 summarises the analysis of the release permeability data for all six experiments in this study. Columns 2 and 3 give the range of $[Ca_{SR}]_R$ values for the runs used for the analyses (this range also applies to the results in Table 1). Column 4 gives the central value of $[Ca_{SR}]$ for the analysis of release permeability in columns 5–7; the range was ±5 μM of this value (cf. cursors in Fig. 4). Columns 5–7 give the values of k_{Rel}, $\bar{V}_{Rel}$ and Rel_{max}, respectively. The average value of k_{Rel}, 4.7 mV, was not significantly different (Student's paired t test) than the average voltage–steepness factor for Q_γ, 4.3 mV (column 5, 1st section of Table 1). The average value of $\bar{V}_{Rel}$, −45.4 mV, was significantly more

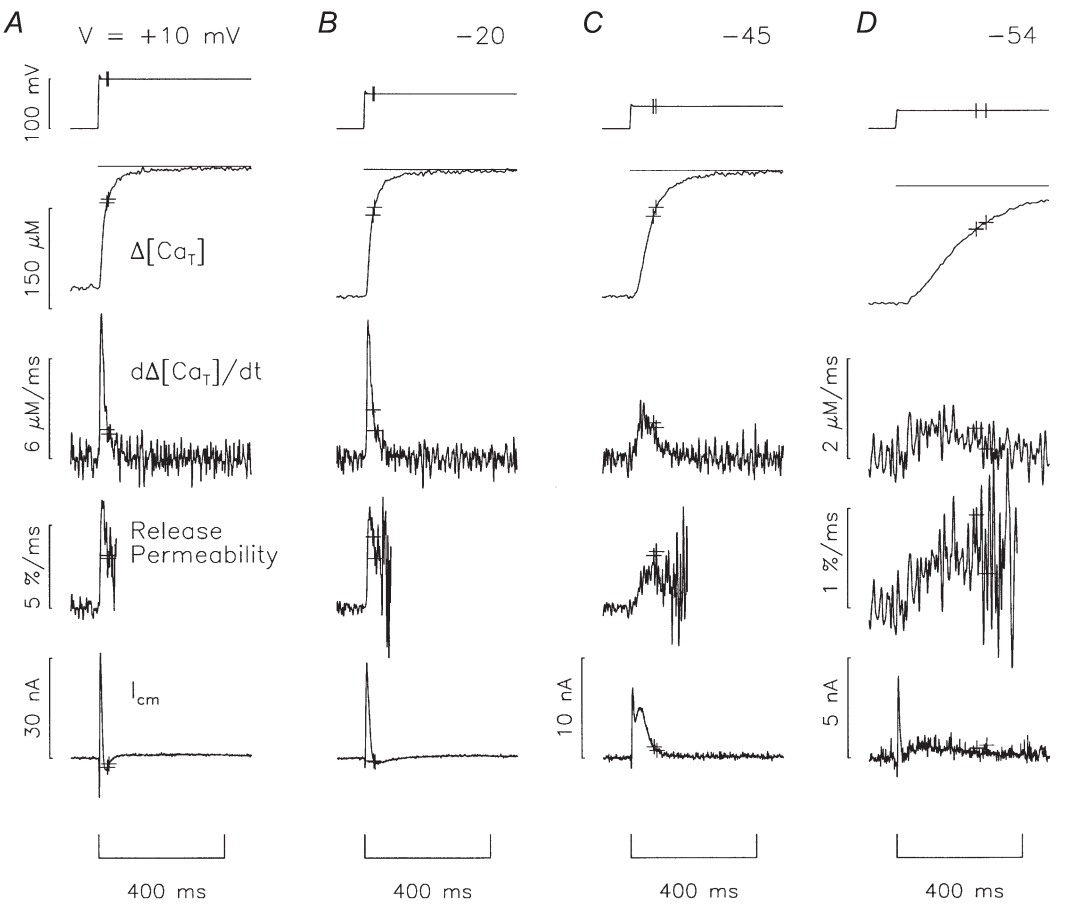

Figure 4. Ca^{2+} release and I_{cm} signals at several voltages

A, the top trace shows a voltage pulse to +10 mV. The next trace shows the $\Delta[Ca_T]$ measured with the EGTA–Phenol Red method. The horizontal line shows $[Ca_{SR}]_R$. The first and second cursors in this and all other traces mark the points when $[Ca_{SR}]$ was reduced to 65 and 55 μM, respectively. The next two traces show the rate of Ca^{2+} release and release permeability signals as indicated. The bottom trace shows I_{cm} calculated with the assumption that $Q_{ON} = -Q_{OFF}$, as described in Methods (also see Fig. 2*C*). The traces in *B*–*D* show analogous traces to those in *A* except that they were obtained with pulses to −20, −45, and −54 mV, respectively. Same experiment as shown in Figs 1–3.

Table 2. Voltage dependence of release permeability

(1)	(2)	(3)	(4)	(5)	(6)	(7)	(8)
	Range of $[Ca_{SR}]_R$ values			Fit of single Boltzmann function			
Fibre	Smallest	Largest	$[Ca_{SR}]$	k_{rel}	$\overline{V}_{Rel}$	Rel_{max}	$\overline{V}_{Rel} - \overline{V}_\gamma$
	(μM)	(μM)	(μM)	(mV)	(mV)	(% ms^{-1})	(mV)
901991	133	248	60	6.9	−42.4	2.42	15.9
913991	171	198	60	4.7	−44.5	3.92	7.3
915991	191	218	60	4.0	−47.0	3.85	5.5
921991	94	115	50	3.5	−49.8	3.26	11.0
923991	40	46	20	2.9	−50.2	2.96	17.1
420001	85	99	50	6.4	−38.5	1.083	14.4
Mean				4.7	−45.4	2.92	12.0
S.E.M.				0.7	1.8	0.43	1.9

Column 1 gives the fibre reference. Columns 2 and 3 give the smallest and largest values of $[Ca_{SR}]_R$, respectively, for the stimulations used to estimate intramembranous charge movement (Table 1) and the voltage dependence of Ca^{2+} release in columns 5–7. The average release permeability for each test pulse in an experiment was determined when $[Ca_{SR}]$ was between ±5 μM of the value in column 4. Columns 5–7 give the parameters of the Boltzmann function fit to the release permeability data calculated as described for column 4. Column 8 gives the difference between $\overline{V}_{Rel}$ in column 6 and $\overline{V}_\gamma$ from column 6 of the first section of Table 1. See text for additional information.

positive than that of $\overline{V}$ for Q_γ, −57.9 mV. The average difference between these values, given in column 8 of Table 2, is 12.0 mV. In summary, the release permeability at small values of $[Ca_{SR}]$ has a steep voltage dependence similar to that of Q_γ and approaches saturation above −40 mV as does Q_γ; its location on the voltage axis, however, is shifted to the right by 12.0 mV on average. As discussed in Discussion, the shift is consistent with multi-state models of the voltage sensor in which some charge moves before a final activating transition.

Comparison of the time courses of Q_γ and Ca^{2+} release

The top trace in Fig. 6A shows a voltage pulse to −54 mV digitally filtered with a 0.01 kHz Gaussian filter. This filter was applied to the remaining traces in this figure in order to reduce noise in the Ca^{2+} release signals. The lower signal in the middle pair of traces shows the measured $\Delta[Ca_T]$ signal. The constant line shows $[Ca_{SR}]_R$. The earlier, noisier trace in the bottom pair of traces is the release permeability. The smoother, delayed trace is Q_γ scaled to have approximately the same final level as the release permeability trace. Q_γ is the integral of I_γ estimated from the I_{cm} trace as described with Fig. 2*C*. It is clear that the release permeability signal precedes Q_γ in apparent contrast to the idea that Q_γ causes Ca^{2+} release.

As given by eqn (A3) in the Appendix, an estimate of the time course of voltage activation (denoted $V_{activation}$) is given by release permeability divided by $[Ca_{SR}]$. The normalisation by $[Ca_{SR}]$ accounts for the expectation that the release permeability decreases during a pulse as $[Ca_{SR}]$, and thereby, calcium-induced calcium release (CICR) decreases. The middle trace in Fig. 6*B* is $[Ca_{SR}]$ ($[Ca_{SR}]_R$ minus $\Delta[Ca_T]$ from *A*), which decreased from about 150 μM at the start of the pulse to near zero at the end (the line shows the zero level). The noisy trace in the bottom pair of traces in Fig. 6*B* shows release permeability divided by $[Ca_{SR}]$, scaled so that its final level matches that of the Q_γ signal (see uncertainty concerning this scaling in next paragraph). It appears that the normalised release permeability trace is delayed with respect to Q_γ, at least after the first 50 ms. The fact that it appears to slightly

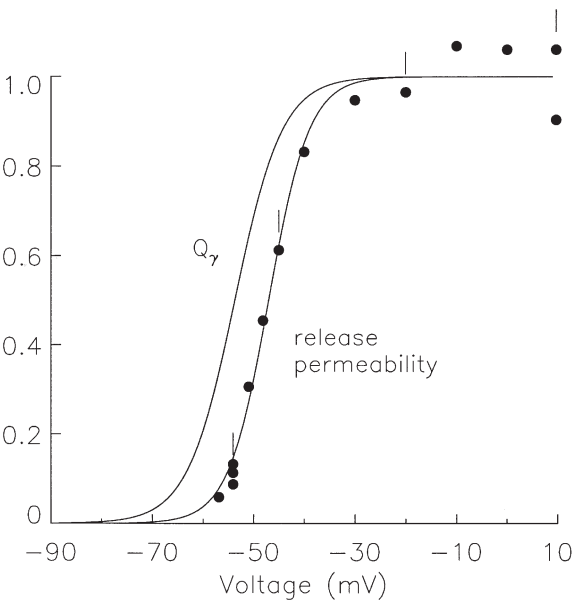

Figure 5. Release permeability and steady-state Q_γ charge *vs.* voltage

The curve on the left plots the Boltzmann function corresponding to the Q_γ component in the fit to the ○s in Fig. 3*A*. The ●s plot the average release permeability when $[Ca_{SR}]$ was between 65 and 55 μM. The points labelled with vertical bars are from the release permeability traces in Fig. 4. The curve through the points is the best fit Boltzmann function to the release permeability data. Same experiment as shown in Figs 1–4.

precede Q_γ for a short period at the start of the pulse could be due to noise in the Ca^{2+} release signal. Another possibility is that some Q_γ charge actually does move in the first 23 ms in contrast to the assumption used for the estimation of Q_γ (see Fig. 2*C*).

It is important to note that there is some uncertainty in the value of $[Ca_{SR}]_R$ and that even a small error could result in a relatively large error in the final value of $[Ca_{SR}]$. Since the normalised release permeability trace is actually the rate of release divided by the square of $[Ca_{SR}]$, there is even more uncertainty in its final level, and, thereby, the scale factor applied to the normalised release permeability signal for its comparison with the Q_γ signal (see above). For this reason and because of the various assumptions involved and the poor signal to noise of the normalised release permeability signal, the result in Fig. 6*B* should be considered as weak evidence, at best, of a lag between Q_γ and voltage activation of Ca^{2+} release. Therefore, the question remains open as to whether or not a lag is present, an apparent requirement if Q_γ causes Ca^{2+} release (see Discussion). This analysis does, however, indicate that changes in CICR will probably need to be considered if this question is re-examined at a later date.

DISCUSSION

The component identified as Q_γ in this study includes contributions from an additional slow component of charge movement

The values of steady-state intramembranous charge in this study can be compared with those of Hui & Chandler (Table III, columns 5–7; 1990), also obtained with Cl^- in the external solution and an internal solution containing caesium glutamate and 20 mM EGTA. The average value of q_{max}/c_m for the Q_γ component of ~30 nC μF^{-1} in this study (all three sections of Table 1) is much larger than their value of 13.2 nC μF^{-1}. One reason is that the non-linear ionic component was estimated with sloping baselines in the earlier study, whereas a constant baseline was used in

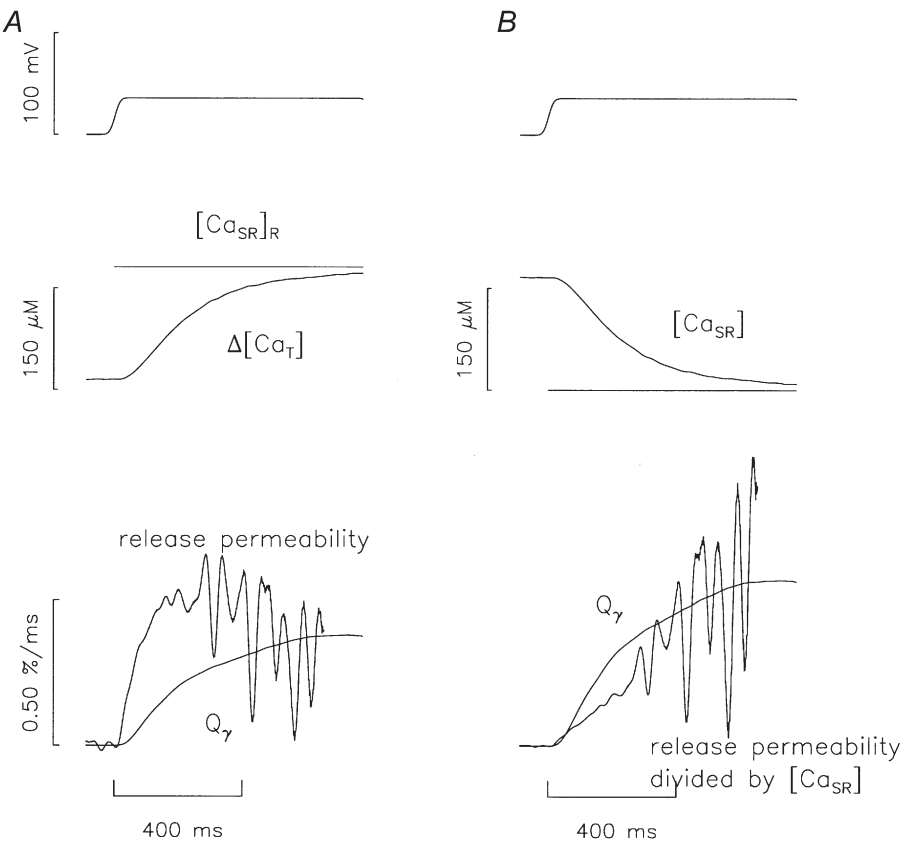

Figure 6. Time course of voltage activation and Q_γ charge

A, the top trace shows a voltage step to −54 mV digitally filtered with a cut off frequency of 0.01 kHz (see Methods). The same filter was applied to all the other traces in this figure. The bottom signal in the next pair of traces shows $\Delta[Ca_T]$ and the constant line shows $[Ca_{SR}]_R$ (note that the maximum in the $\Delta[Ca_T]$ trace occurred later in the stimulation protocol). The noisy trace in the bottom pair of traces is the release permeability signal and the other trace is Q_γ. *B*, the top trace is the same voltage trace shown in *A*. The next trace shows $[Ca_{SR}]$ given by $[Ca_{SR}]_R - \Delta[Ca_T]$ in *A*. The line shows the zero level. The noisy trace in the bottom pair of traces is the release permeability signal divided by $[Ca_{SR}]$. The other trace is Q_γ from *A* scaled so that its final value approached that of the normalised release permeability signal. See text for details. Same experiment as shown in Figs 1–5.

this study (a sloping baseline typically yields 20–40 % less charge in our records). The probable explanation for most of the extra charge is that the pulse durations in this study were 600 ms *vs.* 200 ms in Hui & Chandler. In support of this explanation, Pape *et al.* (1996, Table 1) found a greater than 2-fold increase in q_{max}/c_m obtained from fitting a single Boltzmann distribution function to data obtained with 700–800 ms pulses *vs.* data obtained with 300–400 ms pulses (with gluconate instead of Cl^- as the external anion). It was suggested that either additional charge moves after 300–400 ms or that some change in ionic conductance occurs which somehow increases the OFF Q_{cm} values. The latter explanation seems less likely, since the $I_{test} - I_{control}$ traces with the gluconate solution appear to have almost no ionic component. Even if this late charge is associated with the Q_γ component, it presents a potential problem in this study since the release permeability values at the more depolarised potentials were obtained before most of this late charge had moved (see Fig. 4).

The average values of $\overline{V}$ and k for the Q_γ component of charge in Hui & Chandler (1990; Table 3, columns 5 and 6) were −56.5 mV (S.E.M. = 1.3; n = 10) and 2.9 mV (S.E.M. = 0.4), respectively, and they were −57.4 mV and +4.3 mV in this study (1st section of Table 1). The values of $\overline{V}$ are very similar and not significantly different whereas the value of k was significantly greater in this study. The values of k are relatively close, however, with significant overlap between the two ranges of values, 1.4–4.7 mV in Hui & Chandler, *vs.* 2.8–5.2 mV in this study. Assuming that the pulse duration is the only difference between the two studies, this result suggests that the late component of charge produces only a small increase in k and little or no change in $\overline{V}$. This is important since $\overline{V}$ and k (and not q_{max}/c_m) are the only parameters defining the functional form of the normalised Q_γ *vs.* voltage relationship used for the comparison with that of release permeability (Fig. 5 and Tables 1 and 2). Since the aim in this study is to make only a semi-quantitative comparison, possible errors due to the late charge are apparently too small to influence the conclusions below.

Relationship between release permeability and Q_γ

A main finding in this study is that the average voltage steepness factor of release permeability, 4.7 mV (column 5 of Table 2), is very close to that for Q_γ, 4.3 mV (column 5, Table 1), based on results from the full voltage range from −70 to +10 mV. In addition, the release permeability, like Q_γ, approaches a maximum as voltage is increased above −40 mV. The $\overline{V}$ for release, however, was significantly more positive, by an average of 12 mV .

The voltage shift of Ca^{2+} release compared to Q_γ can be explained by a multiple-state model (3 or more states) of the voltage sensor in which charge moves during transitions between non-activating states. An example is given by the model of Jong *et al.* (1995*b*) developed to account for the kinetics of Q_γ in the absence of Ca^{2+} release. This model assumes that the voltage sensor is composed of four identical subunits that interact co-operatively and that all four subunits must move in order to activate Ca^{2+} release. As is the case of the experimental data in this study (Fig. 5 and Tables 1 and 2), the voltage steepness factors of the release permeability and Q_γ predicted with the model are very similar to each other (determined with the model parameters given in Fig. 14*B* of Jong *et al.* 1995*b*). The voltage shift predicted by the model, 7.9 mV, is also similar to the experimentally determined average value of 12.0 mV in column 8 of Table 2. The voltage dependence of Q_γ and Ca^{2+} release predicted by the model, however, are less steep and the time course of Q_γ at −54 mV was much earlier than that observed in this study. These differences can be attributed to the fact that the model parameters were adjusted to provide a semi-quantitative match to data obtained with gluconate instead of Cl^- as the external anion. It is important to note that this is not the only proposed multi-state model that can account for the voltage shift. It appears that none of the current models, however, can account for both the kinetics and steady-state properties of Q_γ and Ca^{2+} release reported in this study without major adjustments.

Comparison with results from other laboratories

Melzer *et al.* (1986) and Simon & Hill (1992) also compared calcium release and intramembranous charge movement signals in frog skeletal muscle over a large range of voltages. Both of these studies produced somewhat similar results to those presented here, namely that the voltage dependence of Ca^{2+} release is shifted to the right compared to that of charge movement. Due to differences in experimental conditions and methods and interpretations of charge movement and the Ca^{2+} release signals, however, it is difficult, if not impossible, to relate the results and interpretation of the data in their studies with those reported here. One of these differences is that clear Q_γ 'hump' components were not observed in their studies and information about the Q_γ *vs.* the Q_β component was not obtained. In addition, Ca^{2+} release, estimated from free Ca^{2+} transients measured with the Ca^{2+} indicator dye antipyrylazo III was not detected for voltages < -40 mV whereas measurable release signals were detected at −70 mV with the more sensitive EGTA–Phenol Red method used in this article. If Ca^{2+} release is undetected because of insensitivity of the method employed, this should produce an apparent shift to the right of the voltage dependence of Ca^{2+} release. In addition the voltage dependence of Ca^{2+} release in their studies was very likely influenced by Ca inactivation. Although these and other problems might preclude any inferences about the voltage activation of Ca^{2+} release from their data at this later date, it should be acknowledged that Simon & Hill (1992) also proposed that a voltage sensor contains several particles, all of which must move for its associated SR Ca^{2+} release

channel to open. In any case, the results in this article could be considered as stronger evidence in support of this idea.

Is the decline in release permeability due to Ca^{2+} inactivation or a reduction in CICR?

With the constraint that some charge moves during non-activating transitions (see above), it appears that the time course of voltage activation of Ca^{2+} release must lag that of Q_γ if Q_γ causes Ca^{2+} release. A critical assumption in the assessment of whether or not a lag is present in Fig. 6*B* is that the decline in release permeability signal after the peak in Fig. 6*A* is due to a decline in CICR as Ca^{2+} is depleted from the SR. Another possibility, however, is Ca^{2+} inactivation, which is known to produce a rapid decline in the release permeability signal after its peak when $[Ca_{SR}]$ is relatively large. One observation indicates that Ca^{2+} inactivation is, at least, greatly reduced in this study. The exponential time constant for the rate of decline of the release permeability signals associated with the pulse to −20 mV in Fig. 4*B* is estimated to be ~35 ms (fit not shown). This value is much greater than the 2–3 ms time constants obtained with normal SR Ca^{2+} loads ($[Ca_{SR}] \sim 2000\ \mu M$) and attributed to Ca^{2+} inactivation of Ca^{2+} release (Jong *et al.* 1995*a*). Other evidence summarised in Pape *et al.* (1998; p. 280) also suggests that Ca^{2+} inactivation is greatly reduced and perhaps eliminated at the reduced $[Ca_{SR}]$ values present in this study.

One check of the idea that the declining phase of the release permeability signal is due a decline in CICR is to assess whether the time course of the decline is consistent with this idea. If the idea is correct, eqns (A1) and (A2) in Appendix indicate that the time course of the declining phase of the release permeability signal should match that of $[Ca_{SR}]$ near the end of a long pulse, after voltage activation is complete. As is evident from signals in Fig. 4, the declining phases of release permeability signals become slower as the voltage pulse becomes more negative as do those of $[Ca_{SR}]$ (given by $[Ca_{SR}]_R - \Delta[Ca_T]$). A quantitative comparison (not shown) indicates that the exponential time constants of the declining phases of the release permeability signals are in fact similar to those of the latter part of the corresponding $[Ca_{SR}]$ signals. This correspondence supports the idea that the declining phase of the release permeability signal is due to a decrease in CICR with decreasing $[Ca_{SR}]$ rather than Ca^{2+} inactivation, though some contribution by Ca^{2+} inactivation or some other process cannot be ruled out.

As noted with Fig. 6*B*, the question as to whether or not a lag is present remains unresolved, in part because of this uncertainty about the cause of the declining phase of the release permeability.

Is $CICR_{activation}$ independent of voltage?

As explained in Appendix (see eqns (A1) and (A2)), earlier results support a simple model in which release permeability is given by the product of a voltage activation factor (denoted $V_{activation}$) and a factor for CICR (denoted $CICR_{activation}$) that is proportional to $[Ca_{SR}]$. In order to have about the same contribution by $CICR_{activation}$ at every voltage, the release permeability values were estimated at the same value of $[Ca_{SR}]$ within each experiment (cursors in Fig. 4, Table 2, column 4). With a constant $CICR_{activation}$, release permeability should be proportional to $V_{activation}$ thereby allowing its apparently straightforward comparison with Q_γ. It is possible, however, that $CICR_{activation}$ is still somehow dependent upon voltage even at constant $[Ca_{SR}]$.

As mentioned in Introduction, Ca^{2+} release at low levels of depolarisation occurs at voltage-activated sites whose state of activation should not be affected by Ca^{2+} from neighbouring sites due to the relatively large separation between sites and the Ca^{2+} buffering of EGTA. This does not rule out the possibility that a Ca^{2+} release channel activated by its associated voltage sensor is somehow regulated by Ca^{2+}. Another possibility is that each voltage-activated site is composed of a single voltage-activated channel and neighbouring channels recruited by CICR as proposed by Ríos and colleagues (Shirokova *et al.* 1996; Shirokova & Ríos, 1997; Stern *et al.* 1997). Even if either or both of these situations occurs, $CICR_{activation}$ could still be independent of voltage if the effect of voltage is to regulate the density of such voltage-activated sites without altering the extent of activation by CICR within each site. Results of Klein *et al.* (1997) suggest that this is in fact the case, at least with fibres having a normal SR Ca^{2+} load. They observed Ca^{2+} sparks in fibres in which most of the voltage sensors were immobilised in order to greatly reduce spatial overlap between Ca^{2+} sparks at larger voltages. The duration and amplitude of Ca^{2+} sparks were essentially independent of voltage. As a result, the main effect of voltage on the global Ca^{2+} release was to regulate the density of Ca^{2+} sparks as opposed to spark properties. If the same conclusion applies to the global Ca^{2+} release signals in this study, $CICR_{activation}$ would be independent of voltage.

It is important to note that the results of Klein *et al.* (1997) were obtained with a presumably normal calcium load and they indicated that most Ca^{2+} sparks were likely terminated by Ca^{2+} inactivation. With the small values of $[Ca_{SR}]$ in this study, release from a Ca^{2+}-release channel could terminate by the return of its associated voltage sensor to an inactive state or when Ca^{2+} comes off an activation site or by Ca^{2+} inactivation, if present. It is possible, therefore, that spark properties vary with voltage when $[Ca_{SR}]$ is small. Although this would not necessarily imply that $CICR_{activation}$ also varies with voltage, it is possible, for example that the extent of activation of neighbouring channels depends on Ca^{2+} spark duration. The results of Klein *et al.* (1997) also do not rule out saturation of activated Ca^{2+} release channels as the density of voltage-activated sites

with neighbouring Ca^{2+}-activated channels increases with voltage in the absence of charge immobilisation.

In summary, Ca^{2+} may have influenced the functional form of release permeability *vs.* voltage even though $[Ca_{SR}]$ was the same at each voltage. Although the results in this article provide additional evidence in support of the idea that Q_γ causes Ca^{2+} release, they fall short of proving it for this and other reasons mentioned above.

APPENDIX

Simple model of voltage activation and CICR when $[Ca_{SR}]$ is < 250 μM

This appendix describes a simple model of activation of Ca^{2+} release by both voltage and CICR when $[Ca_{SR}]$ is < 250 μM. The model is motivated by earlier results indicating that release permeability increases approximately linearly with $[Ca_{SR}]$ when $[Ca_{SR}]$ increases from < 100 to ~300 μM for voltage steps from −70 to −60 mV (P. C. Pape & N. Carrier, 1998) and to −45 mV (P. C. Pape & N. Carrier, unpublished observations); the linear relationship at each voltage extrapolates to about zero as $[Ca_{SR}]$ approaches zero. Based on a similarity with analogous results from isolated SR Ca^{2+} release channels reconstituted in bilayers (Tripathy & Meissner, 1996), Pape & Carrier (1998) attributed the increase to CICR. A simple way to account for the results in voltage-clamped fibres is to assume that:

$$\text{Release permeability} \propto V_{\text{activation}} \times CICR_{\text{activation}}, \quad \text{(A1)}$$

where $V_{\text{activation}}$ is the extent of activation of Ca^{2+} release channels by voltage and $CICR_{\text{activation}}$ is the extent of activation (modulation) by calcium-induced Ca^{2+} release and that:

$$CICR_{\text{activation}} \propto [Ca_{SR}]. \quad \text{(A2)}$$

Equation (A1) might appear to be impossible; if Ca^{2+} involved in $CICR_{\text{activation}}$ can only come from an open channel, the channel would never open. This problem can be circumvented by assuming that a SR Ca^{2+} release channel activated by voltage can open, if only for a very short time, even in the absence of Ca^{2+} release. The time is too short, however, to produce detectable Ca^{2+} release.

Assuming that there is no lag between $CICR_{\text{activation}}$ and $[Ca_{SR}]$, the time course of $V_{\text{activation}}$ during a pulse would be given by:

$$V_{\text{activation}} \propto \text{release permeability} \div [Ca_{SR}]. \quad \text{(A3)}$$

The assumption of no lag between $CICR_{\text{activation}}$ and $[Ca_{SR}]$ can be evaluated from the rate constant of Ca^{2+} binding to and dissociation from the calcium activation site in isolated SR Ca^{2+} release channels. In experiments involving rapid increases in $[Ca^{2+}]$ to 1 μM in the vicinity of a single SR Ca^{2+} release channel in a bilayer by flash photolysis of caged Ca^{2+}, Györke *et al.* (1994) estimated that Ca^{2+} binds to the activation site with a maximum time constant of 1.43 ms. This result corresponds to an ON rate constant for calcium binding of 0.7×10^8 $M^{-1}s^{-1}$. Taking into account the presence of MgATP in the internal solution, the K_D for Ca^{2+} binding to the activation site is estimated to be ~5 μM (personal communication by Gerhard Meissner). From the ON rate constant and K_D, the OFF rate constant for calcium is estimated to be ~350 s^{-1} which corresponds to a time constant of ~3 ms. As a check, this OFF time constant is in the range of mean open times of isolated SR Ca^{2+} release channels in bilayers activated by calcium and likely closed when calcium leaves the activation site (Tripathy & Meissner, 1996). These results indicate that the time constant for the delay between changes in $CICR_{\text{activation}}$ and $[Ca_{SR}]$ should be less than ~3 ms. The use of eqn (A3) is to determine the time course of $V_{\text{activation}}$ for comparison with that of Q_γ in Fig. 6*B*. Since $[Ca_{SR}]$ in Fig. 6*B* decreases relatively slowly (exponential time constant of ~180 ms) compared to this 3 ms time constant, the assumption of no lag between $CICR_{\text{activation}}$ and $[Ca_{SR}]$ for eqn (A3) should be valid.

It is noted that Ashley & Moisescu (1973; see also Ashley *et al.* 1974) were the first to propose, to our knowledge, that the rate of Ca^{2+} release from the SR is the product of two terms, one accounting for activation by voltage and the other by CICR. Their conclusion was based on modelling of Ca^{2+} binding to myoplasmic sites and reuptake into the SR by the calcium pump, all driven by the free calcium transient estimated with the Ca^{2+} indicator aequorin. As this was an indirect approach dependent upon several assumptions and did not account for Ca^{2+} depletion of the SR during release, Ca^{2+} inactivation of Ca^{2+} release, or the time course of voltage activation (none of which were known at the time), the work of Ashley and colleagues should not be considered as strong support of eqn (A1).

REFERENCES

Adrian, R. H. & Peres, A. (1979). Charge movement and membrane capacity in frog muscle. *Journal of Physiology*. **289**, 83–97.

Ashley, C. C. & Moisescu, D. G. (1973). The mechanism of the free calcium change in single muscle fibres. *Journal of Physiology* **231**, 23–25*P*.

Ashley, C. C. & Moisescu, D. G. (1974). Kinetics of calcium during contraction: myofibrillar and SR fluxes during a single response of a skeletal muscle fibre. In *Calcium Binding Proteins,* ed. Drabikowski, W. *et al.*, pp. 609–642. Elsevier, Amsterdam.

Baylor, S. M., Chandler, W. K. & Marshall, M. W. (1983). Sarcoplasmic reticulum calcium release in frog skeletal muscle fibers estimated from arsenazo III calcium transients. *Journal of Physiology* **334**, 625–666.

Chandler, W. K. & Hui, C. S. (1990). Membrane capacitance in frog cut twitch fibers mounted in a double Vaseline-gap chamber. *Journal of Physiology* **96**, 225–256.

Colquhoun, D.& Sigworth, F. J. (1983). Fitting and statistical analysis of single-channel records. In *Single-Channel Recording*, ed. Sakmann, B. & Neher, E., pp. 191–263. Plenum Publishing Corp., New York.

Csernoch, L., Pizarro, G., Uribe, I., Rodriguez, M. & Ríos, E. (1991). Interfering with calcium release suppresses I_γ, the 'hump' component of intramembranous charge movement in skeletal muscle. *Journal of General Physiology* **97**, 845–884.

Donoso, P., Prieto, H. & Hidalgo, C. (1995). Luminal calcium regulates calcium release in triads isolated from frog and rabbit skeletal muscle. *Biophysical Journal* **68**, 507–515.

García, J., Pizarro, G., Ríos, E. & Stefani, E. (1991). Effect of the calcium buffer EGTA on the 'hump' component of charge movement in skeletal muscle. *Journal of General Physiology* **97**, 885–896.

Györke, S., Vélez, P., Suárez-Isla, B. & Fill, M. (1994). Activation of single cardiac and skeletal ryanodine receptor channels by flash photolysis of caged Ca^{2+}. *Biophysical Journal* **66**, 1879–1886.

Hille, B. & Campbell, D. T. (1976). An improved Vaseline gap voltage clamp for skeletal muscle fibers. *Journal of General Physiology* **67**, 265–293.

Hodgkin, A. L. & Horowicz, P. (1960). Potassium contractures in single muscle fibres. *Journal of Physiology* **153**, 386–403.

Horowicz, P. & Schneider, P. (1981). Membrane charge moved at contraction thresholds in skeletal muscle fibres. *Journal of Physiology* **314**, 595–633.

Huang, C. L.-H. (1982). Pharmacological separation of charge movement components in frog skeletal muscle. *Journal of Physiology* **324**, 375–387.

Hui, C. S. (1983). Pharmacological studies of charge movement components in frog skeletal muscle. *Journal of Physiology* **337**, 509–529.

Hui, C. S. & Chandler, W. K. (1990). Intramembranous charge movement in frog cut twitch fibers mounted in a double Vaseline-gap chamber. *Journal of General Physiology* **96**, 257–297.

Hui, C. S. & Chandler, W. K. (1991). Q_β and Q_γ components of intramembranous charge movement in frog cut twitch fibers. *Journal of General Physiology* **98**, 429–464.

Hui, C. S. & Chen, W. (1994). Origin of delayed outward ionic current in charge movement traces from frog skeletal muscle. *Journal of Physiology* **479**, 109–125.

Jong, D.-S., Pape, P. C. & Chandler, W. K. (1995*a*). Calcium inactivation of calcium release in frog cut muscle fibers that contain millimolar EGTA or fura-2. *Journal of General Physiology* **106**, 337-388.

Jong, D.-S., Pape, P. C. & Chandler, W. K. (1995*b*). Effect of sarcoplasmic reticulum calcium depletion on intramembranous charge movement in frog cut muscle fibers. *Journal of General Physiology* **106**, 659–704.

Klein, M. G., Cheng, H., Santana, L. F., Jiang, Y.-H., Lederer, W. J. & Schneider, M. F. (1996). Two mechanisms of quantized calcium release in skeletal muscle. *Nature* **379**, 455–458.

Klein, M. G., Lacampagne, A. & Schneider, M. F. (1997). Voltage dependence of the pattern and frequency of discrete Ca^{2+} release events after brief repriming in frog skeletal muscle. *Proceedings of the National Academy of Sciences of the USA* **94**, 11061–11066.

MacLennan, D. H. & Wong, P. T. S. (1971). Isolation of a calcium-sequestering protein from sarcoplasmic reticulum. *Proceedings of the National Academy of Sciences of the USA.* **68**, 1231–1235.

Maylie, J., Irving, M., Sizto, N.-L. & Chandler, W. K. (1987). Comparison of arsenazo III optical signals in intact and cut frog twitch fibers. *Journal of General Physiology* **89**, 41–81.

Melzer, W., Schneider, M. F. Simon, B. J. & Szúcs, G. (1986). Intramembranous charge movement and calcium release in frog skeletal muscle. *Journal of Physiology.* **373**, 481–511.

Miledi, R., Nakajima, S., Parker, I. & Takahashi, T. (1981). Effects of membrane polarization on sarcoplasmic reticulum calcium release in skeletal muscle. *Proceedings of the Royal Society of London* B **213**, 1–13.

Mobley, B. A. & Eisenberg, B. R. (1965). Sizes of components in frog skeletal muscle measured by methods of stereology. *Journal of General Physiology* **66**, 31–45.

Pape, P. C. & Carrier, N. (1998). Effect of sarcoplasmic reticulum (SR) calcium content on SR calcium release elicited by small voltage-clamp depolarizations in frog cut skeletal muscle fibers equilibrated with 20 mM EGTA. *Journal of General Physiology* **112**, 161–179.

Pape, P. C., Jong, D.-S. & Chandler, W. K. (1995). Calcium release and its voltage dependence in frog cut muscle fibers equilibrated with 20 mM EGTA. *Journal of General Physiology* **106**, 259-336.

Pape, P. C., Jong, D.-S. & Chandler, W. K. (1996). A slow component of intramembranous charge movement during sarcoplasmic reticulum calcium release in frog cut muscle fibers. *Journal of General Physiology* **107**, 79–101.

Pape, P. C., Jong, D.-S. & Chandler, W. K. (1998). Effects of partial sarcoplasmic reticulum calcium depletion on calcium release in frog cut muscle fibers equilibrated with 20 mM EGTA. *Journal of General Physiology* **112**, 263–295.

Pizarro, G., Csernoch, L., Uribe, I., Rodriguez, M. & Ríos, E. (1991). The relationship between Q_γ and Ca^{2+} release from the sarcoplasmic reticulum calcium release in frog cut muscle fibers. *Journal of General Physiology* **97**, 913–947.

Prieto, H., Donoso, P., Rodriguez, P. & Hidalgo, C. (1994). Intraluminal calcium affects markedly calcium release rates in triads from rabbit but not from frog. *Biophysical Journal* **66**, A339.

Schneider, M. F. & Chandler, W. K. (1973). Voltage dependent charge movement in skeletal muscle: a possible step in excitation–contraction coupling. *Nature* **242**, 244–246.

Schneider, M. F. & Simon, B. J. (1988). Inactivation of calcium release from the sarcoplasmic reticulum in frog skeletal muscle. *Journal of Physiology* **405**, 727–745.

Shirokova, N., Garcia, J., Pizarro, G. & Ríos, E. (1996). Ca^{2+} release from sarcoplasmic reticulum compared in amphibian and mammalian skeletal muscle. *Journal of General Physiology* **107**, 1–18.

Shirokova, N., & Ríos, E. (1997). Small event Ca^{2+} release: a probable precursor of Ca^{2+} sparks in frog skeletal muscle. *Journal of Physiology* **502**, 3–11.

Simon, B. J. & Hill, D. A. (1992). Charge movement and SR calcium release in frog skeletal muscle can be related by Hodgkin–Huxley model with four gating particles. *Biophysical Journal* **61**, 1109–1116.

Stern, M. D., Pizarro, G.& Ríos, E. (1997). Local control model of excitation–contraction coupling in skeletal muscle. *Journal of General Physiology* **110**, 415–440.

Szucs, G., Csernoch, L., Magyar, J. & Kovacs, L. (1991). Contraction threshold and the 'hump' component of charge movement in frog skeletal muscle. *Journal of General Physiology* **97**, 897–911.

Tripathy, A. & Meissner, G. (1996). Sarcoplasmic reticulum lumenal Ca^{2+} has access to cytosolic activation and inactivation sites of skeletal muscle Ca^{2+} release channel. *Biophysical Journal* **70**, 2600–2615.

Vergara. J. & Caputo, C. (1983). Effects of tetracaine on charge movement and calcium signals in frog skeletal muscle fibers. *Proceedings of the National Academy of Sciences of the USA* **80**, 1477–1481.

Acknowledgements

This work was supported by the Canadian Institutes of Health Research grant MT-12552 and a grant from Fonds de la recherche en santé du Québec.